



Effects of petrographic and diagenetic characteristics on reservoir quality of Late Cretaceous Abu Roash “G” Member, Abu Sennan area, Western Desert, Egypt

Ghada Farrag¹ · Osama Elnaggar² · Zakaria Hassan³ · Ashraf Baghdady⁴

Received: 16 February 2022 / Accepted: 13 May 2022 / Published online: 25 May 2022
© Saudi Society for Geosciences 2022

Abstract

The main purpose of this work is to assess the sedimentological characteristics and their effect on reservoir quality of the oil/gas producer Abu Roash “G” Member (Late Cenomanian) in Abu Sennan area, north Western Desert, Egypt. Abu Roash “G” Member is subdivided into three units: the lower, middle, and upper. Petrographically, the lower unit composed of quartz wacke, lithic graywacke, pack-wackestone, shale, silty shale, quartz arenite, and sandy calcareous shale. The middle unit consists of calcareous shale, silty shale, and sandy shale. On the other hand, the upper unit is dominated by sandy shale, shale, and quartz arenite. These microfacies association suggests shallow marine depositional environment. This member was subjected to different types of diagenetic process such as compaction, biogenic alteration, dissolution, cementation, and neomorphism. Some of these processes lead to porosity enhancement such as dissolution, while the later-on filling of the fractures by silica/calcite destructs the reservoir quality. This is because the resulted fractures are filled later by calcite/silica minerals. The sedimentological characteristics witnessed the heterogeneity of the Abu Roash “G” Member as a result of depositional setting and diagenesis. Petrophysically, the Abu Roash “G” Member is a heterogeneous reservoir in terms of fluid flow properties, where three flow units with different capabilities are involved. Reservoir performance would be different among the contained microport, mesoport, and macroport flow units.

Keywords Late Cretaceous · Abu Roash “G” · Depositional environment · Diagenesis · Western Desert

Responsible Editor: Attila Ciner

✉ Ghada Farrag
geol.ghada@gmail.com

Osama Elnaggar
osama_221@yahoo.com

Zakaria Hassan
tbondoc2@gmail.com

Ashraf Baghdady
arbaghdady@sci.asu.edu.eg

¹ Exploration Department, General Petroleum Company, Cairo, Egypt

² Production Department, Egyptian Petroleum Research Institute (EPRI), Cairo, Egypt

³ Geology Department, Faculty of Science, Cairo University, Cairo, Egypt

⁴ Geology Department, Faculty of Science, Ain Shams University, Cairo 11566, Egypt

Introduction

Abu Sennan area is located in the central part of Abu Gharadig basin, north Western Desert, Egypt. It includes three oil fields, namely SWS, GPT, and GPY (Fig. 1). The structural configuration of Abu Sennan area is represented by a group of en’echelon normal faults with NE-SW orientation formed during Jurassic time in response to NW–SE extension. These faults are intersected by NW–SE normal faults that formed in the Early Cretaceous time due to another extension stress in the NE-SW orientation. During the Late Cretaceous-Middle Eocene, these NE-SW en’echelon normal faults, suffered from positive structural differential inversion which form the asymmetrical anticlines of Abu Sennan area through 2–3 pulses of inversion (Farrag 2021; Farrag et al. 2021).

The stratigraphic succession of Abu Sennan area (Fig. 2) proposed by GPC (1980) and Farrag et al. (2021) clarified that Abu Roash “G” Member (Late Cenomanian) is conformably overlying Bahariya Formation and

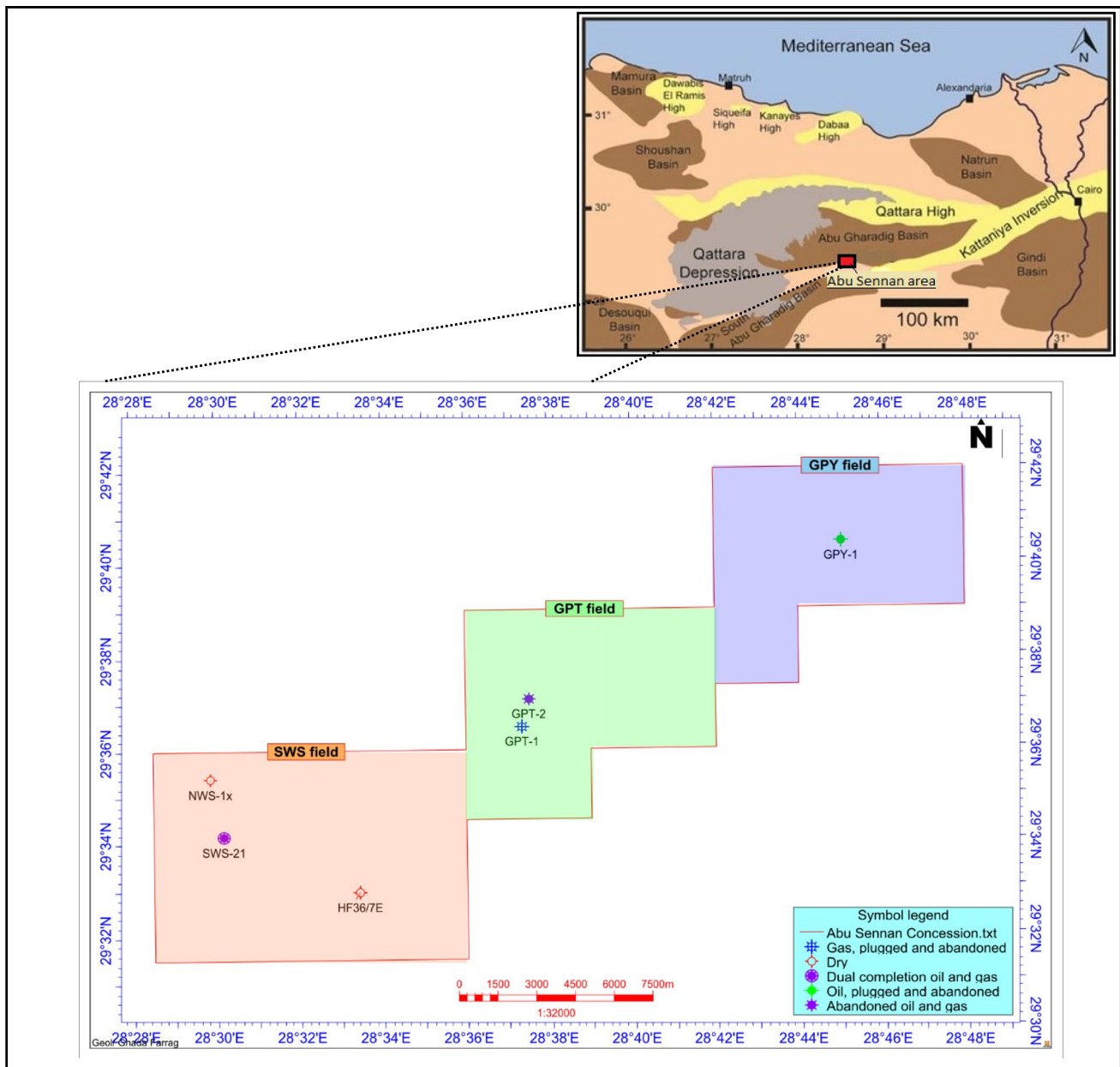


Fig. 1 Location map for the study area showing oilfields (SWS, GPT, and GPY) and studied wells

underlying Abu Roash “F” Member. Abu Roash “G” Member is detected in all studied wells as an oil and gas producer. This member is subdivided into three units: the lower, middle, and upper (Fig. 3). The lower unit of the Abu Roash “G” Member consists of limestone and shale, with silty sandstone interbeds. The middle unit is composed of limestone, shale, and siltstone, with thin sandstone beds, while the upper unit is composed of siltstone and shale, with thin sandstone interbeds.

Many authors have also worked on the facies analysis of the Abu Roash “G” in the Abu Gharadig basin (Pasley et al. 2009; Abdel Gawad et al. 2016; Osman et al. 2017; Bekhit et al. 2017; Sultan et al. 2019).

This paper is focused on facies analysis of the oil/gas producer Abu Roash “G” Member in Abu Sennan area to elucidate the effect of petrographic and diagenetic characteristics on reservoir quality.

Data and methodology

Twenty-four representative thin sections of the Abu Roash “G” Member (Table 1) were petrographically investigated. The thin sections of the sandstones were impregnated by blue dyes for porosity analysis. The investigated sandstones and limestones were classified according to Pettijohn et al. (1987) and Dunham (1962), respectively.

Fourteen core samples are available in the GPT-1 well-handled and subjected to porosity and permeability measurements at the National Research Centre. The core plugs have been shifted to the logs by 15 m (Fig. 3). Washout is very clear in the three wells and increases in the GPY-1 well (bad hole; Fig. 3). This is reflected from the caliper and bit size reading as well as density correction. The GPT-1 and GPY-1 wells were drilled in the eighties; most of the cores were damaged. r35 is used for defining the reservoir flow units in the GPT-1 well in this study.

Results

Microfacies analysis

Lower Abu Roash “G” facies association

Petrographically, it is represented by sandy calcareous shale in the GPY-1 well. This microfacies consists of abundant skeletal grains, minor quartz, and some iron-oxide nodules. They are cemented by sparry calcite and iron oxides with micritic calcite matrix. This rock was subjected to aggrading neomorphism which increased toward the depths from 2406 to 2408 m.

In the SWS-21 well, the Lower Abu Roash “G” Member is represented by (from base to top) pack/wackestone, shale, silty shale, and quartz arenite (Table 1). The allochemical constituents of pack/wackestone are abundant quartz grains and shell fragments with minor iron-oxide nodules. They are embedded in partially recrystallized micritic calcite. The quartz grains are fine sand-sized and angular to sub-angular. Aggrading neomorphism is the most common diagenetic process (Fig. 4a).

Shale is made up of abundant clay minerals, minor quartz, muscovite, and iron-oxide nodules. Iron-oxide cement and fracturing are observed. This shale graded upward to laminated silty shale. Compaction of this rock is manifested by the presence of fractures.

The quartz arenite consists of abundant quartz with some glauconite, muscovite, iron-oxide nodules, and minor feldspars (Fig. 4b). They are cemented by iron oxides with clay matrix. The quartz grains are fine sand-sized, angular to sub-rounded, moderately sorted, and showing straight grain contacts. Dissolution porosity is commonly observed (Fig. 4b). This rock is similar in composition to the sidewall core of

the HF36/7E well (in depth 1861 m), with an exception of the presence of more fine quartz grain.

In the NWS-1x well, two sidewall cores were chosen to represent the Lower Abu Roash “G” Member. These are (from base to top) the quartz wacke and lithic graywacke (Table 1). The quartz wacke is formed of abundant quartz grains embedded in clayey matrix (more than 15%) and cemented by iron oxides. The quartz grains are fine sand-sized, angular, poorly sorted, and displaying straight contacts. The lithic graywacke is formed of abundant quartz, shell rock fragments, glauconite, clays, and rare muscovite (Fig. 4c). The binding materials of this rock are represented by iron-oxide cement and more than 15% clayey matrix. The quartz grains are fine sand-sized, angular, poorly sorted, and showing straight grain contacts.

Middle Abu Roash “G” facies association

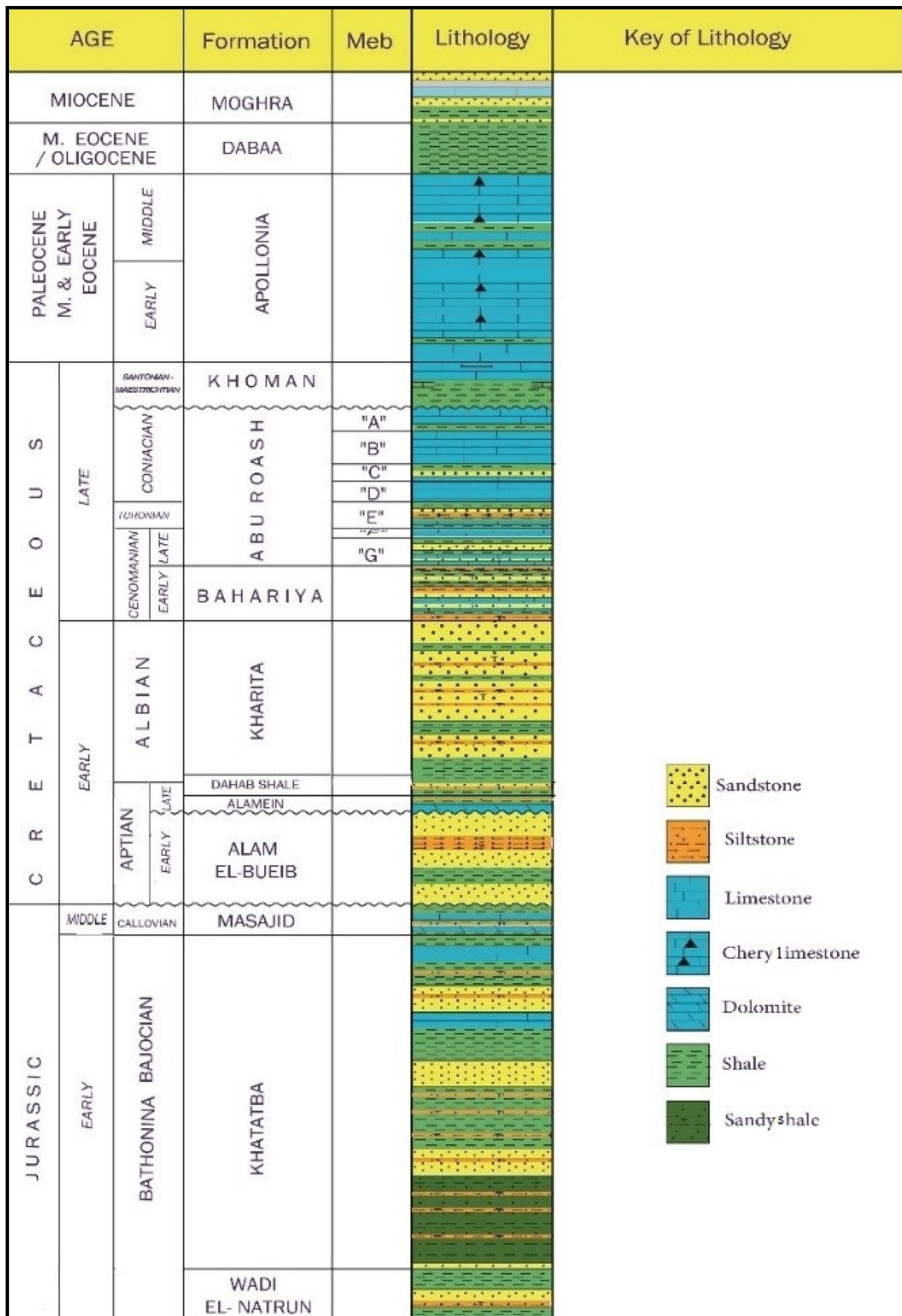
Petrographically, the Middle Abu Roash “G” Member is represented by (from base to top) calcareous shale, silty shale, and sandy shale, in the GPT-1 well. The calcareous shale is formed of skeletal grains (planktonic tests), rock fragments, and iron-oxide nodules cemented by calcite with argillaceous matrix (Fig. 4e). This rock is marked by channel porosity and fissility (Fig. 4d). The silty shale consists of abundant silty-sized angular quartz grains with mica and iron-oxide nodules. They are cemented by iron oxides with argillaceous matrix. This matrix is more abundant than in the sandy shale. Rock fissility, laminations, and fractures are recorded.

The sandy shale consists of abundant quartz, muscovite, and biotite embedded in argillaceous matrix and iron-oxide cement. The quartz grains are very fine sand-sized, angular to sub-angular, and poorly sorted. Dissolution along some fractures is observed. Later, some of these fractures were filled by silica.

Upper Abu Roash “G” facies association

The Upper Abu Roash “G” Member is made up of siltstone and shale, with sandstone thin beds (Fig. 3). Petrographically, the Upper Abu Roash “G” Member is represented (from base to top) by shale, sandy shale, and quartz arenite in the GPT-2 well. The latter microfacies are represented also in the GPT-1 well. The shale is characterized by fissility, fractures, and channel porosity along lamination planes. Later on, the fractures were filled by silica (Fig. 4e).

The sandy shale can be considered as a gradational contact between the upper sand unit and the lower shale unit. It consists of abundant quartz, muscovite, and biotite cemented by iron oxide and embedded in argillaceous matrix. The quartz grains are very fine sand-sized, angular to sub-angular, and poorly sorted. Most of the grains are oriented parallel to lamination planes. This rock was subjected to compaction which



◀**Fig. 2** Generalized stratigraphic successions of Abu Sennan area, north Western Desert (modified after Farrag et al. (2021) and GPC (1980))

caused many fracture sets. Dissolution enhanced the fractures which later on filled by silica (Fig. 4f).

The quartz arenite is composed of abundant quartz grains and iron-oxide nodules with some muscovite flakes and minor feldspars in GPT-1 and GPT-2 wells. They are cemented by iron oxide with less than 15% clayey matrix. At a depth of 1873 m in the GPT-2 well, high Mg-calcite cement is recorded (Fig. 4g). The quartz grains are fine to very fine sand-sized, sub-rounded, and well to moderately sorted. These grains show common straight and rare concavo-convex grain contacts. Rock fracturing witnesses the effect of compaction and filled later by iron oxides.

The sandstone of the Upper Abu Roash “G” Member is represented by sandy shale in the side core (depth 2462.5 m) of the NWS-1 × well (SWS field). It consists of abundant quartz, muscovite, and mica with some glauconite and minor feldspar grains. They are cemented by iron oxides with more than 15% clay matrix. The quartz grains are angular to sub-angular and poorly sorted displaying straight grain contacts. Most of the grains are oriented parallel to lamination planes as in the GPT-2 well. This rock was subjected to compaction leading to fracturing. Dissolution enhanced the fractures and formed channel porosity (Fig. 4h).

Discussion

Diagenetic processes

Diagenesis includes all physical and chemical changes that occurred in sediments after deposition and may be caused by water–rock interactions, microbial activity, and compaction. This process has been divided into eodiagenesis, mesodiagenesis, and telodiagenesis (Choquette and Prey 1970; Abdel Wahab and Turner 1991; Morad et al. 2000; Worden and Burley 2003).

Compaction

In a fine-grained rock, such as shale and siltstone, compaction is usually accompanied by expulsion of interstitial water, reduction in thickness of the bed, and an increase in bulk density (Bjørlykke et al. 2009). The compaction is observed in the shale and silty shale of the Lower Abu Roash “G” Member (SWS-21 well), in addition to the silty shale of the Middle Abu Roash “G” Member (GPT-1 well). The same scenario is present in the sandy shale of the Upper Abu Roash “G” Member (GPT-2 well, Fig. 4f). This process resulted in irregular thickness and

many fractures filled with silica during later stages of diagenesis (mesodiagenesis, Table 2).

Biogenic alteration

Biological diagenesis includes bio-erosion, rasping, boring, and otherwise eroding of rock surfaces by plants and animals. Some organisms may produce secretions that dissolve rock. Bio-erosion is relatively un-important as an agent of change in the carbonate porosity, but it may produce a large percentage of mud fraction in the sediments from some depositional settings (Farrow and Fafe 1988). Bio-erosion through algal attack of the carbonate grains (micritization) is a common process in the studied carbonate rocks. Micritization is a form of degradational neomorphism that causes grain-size reduction. The pack-wackstone of the Lower Abu Roash “G” Member present in the SWS-21 well (SWS field) manifests the effect of biological diagenesis, whereas most of the shell fragments were micritized (Fig. 4a). The biogenic alteration is mainly an eodiagenesis process (Table 2).

Dissolution

Dissolution generally involves the removal in solution of all or part of previously existing minerals, leaving pore spaces in the rocks. It provides silica source for the quartz cement and quartz overgrowth, as well as carbonate source for cements. High temperature under deep burial depth led to the dissolution of some mineral grains at their boundaries (Baiyegunhi et al. 2017). Mineral replacement encompasses dissolution of one mineral and simultaneous precipitation of another mineral in situ. This dissolution and re-precipitation may take place over a time period, with new minerals progressively replacing the host or existing minerals (Baiyegunhi et al. 2017). The dissolution process may be occurred in eo- and telo-diagenesis (Table 2).

The dissolution played an important role in the Abu Roash “G” Member of Abu Sennan area, whereas the quartz arenite present in the SWS-21 well of the Lower/Upper Abu Roash “G” Member is marked by high porosity as a product of dissolution (Fig. 4b). While the sandy shale present in the GPT-1 well of the Middle Abu Roash “G” Member, in addition to the NWS-1 × well of the Upper Abu Roash “G” Member are marked by dissolution. This process enhanced fractures which lead to channel porosity. Some of these fractures were filled by silica (Fig. 4e).

Cementation

Cementation is one of the most important processes leading to the transformation of loose sediments into a consolidated rock, thus resulting in porosity reduction. Two types of cements were identified in the sandstones of the Abu Roash

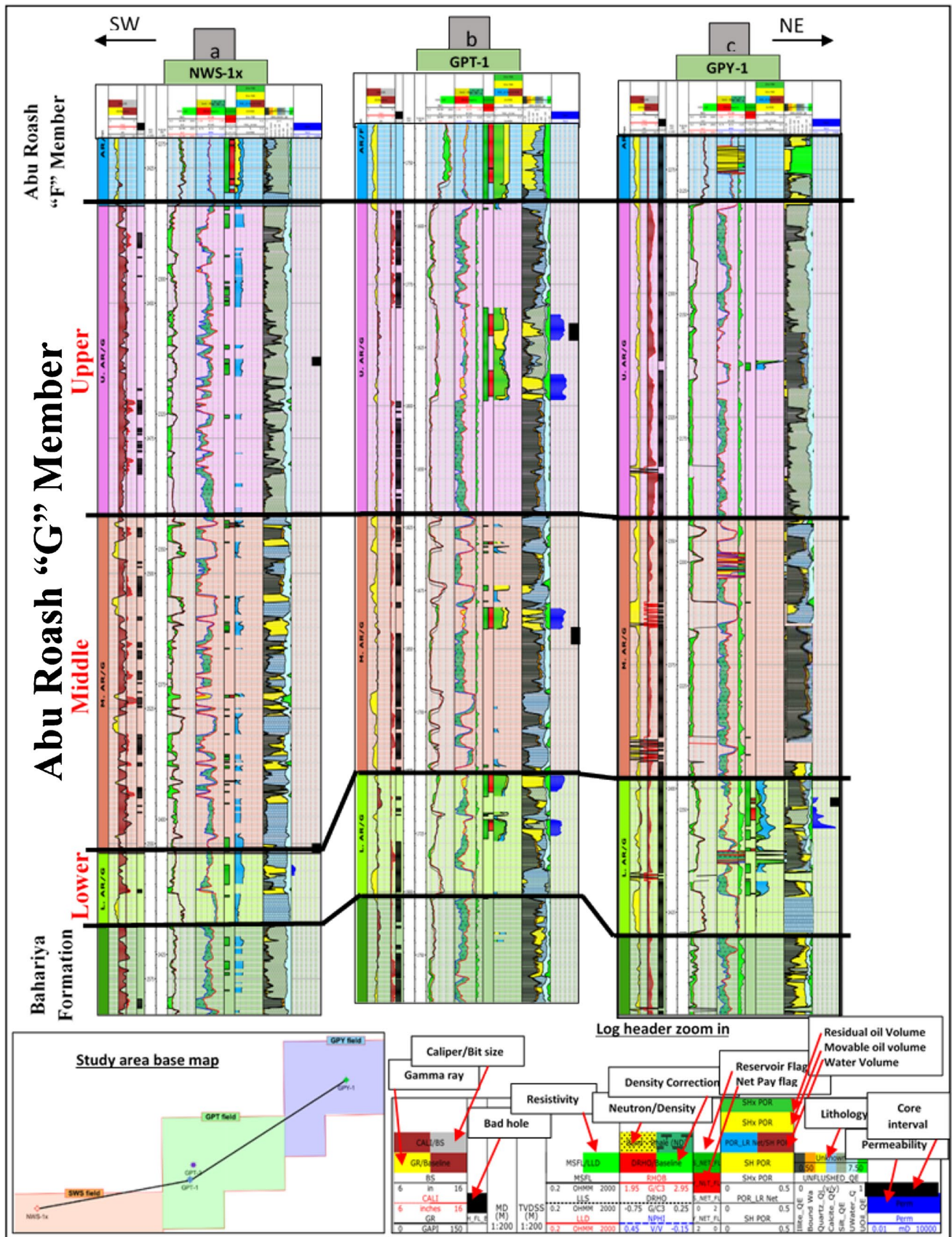


Fig. 3 NE-SW log correlation passing through wells GPY-1, GPT-1, and NWS-1x showing units of the Abu Roash "G" Member in Abu Senna area

Table 1 The selected Abu Roash “G” samples in Abu Sennan area and their microfacies types and measured depth

Member	Unit	Well	No. of samples	Microfacies types	Thin section depths (m)	
Abu Roash “G”	Upper	GPT-1	3	Quartz arenite	1778, 1781, 1784	
			2	Quartz arenite	1870, 1873	
			1	Sandy shale	1877	
	Middle	GPT-1	3	Shale	1878, 1881, 1884	
			1	Sandy shale	2462.5	
			1	Sandy shale	1873	
		Lower	GPY-1	1	Silty shale	1876
				1	Calcareous shale	1879
				3	Sandy calcareous shale	2404, 2406, 2408
	NWS-1x	GPT-1	1	Quartz arenite	1861	
			2	Quartz arenite	1987.5, 1994.5	
			1	Silty shale	1989.5	
			1	Shale	1991.5	
			1	Pack-wackstone	1992.5	
			1	Lithic grey wacke	2541	
			1	Quartz wacke	2543	

“G” Member in Abu Sennan area, which are calcite, and iron oxides. Calcite cement is clearly observed in the calcareous shale present in the GPT-1 well of the Middle Abu Roash “G” Member (Fig. 4e). In some cases, the cement penetrates the grains. Also, calcite cement replaces quartz overgrowths (Burley and Kantorowicz 1986). Generally, calcite cement filled most of the secondary pores after feldspar dissolution.

Iron-oxide cements are present in three different forms: (i) as pervasive pore filling, which is the most common, (ii) as occasional patches, and (iii) as thin coating around detrital grain boundary which is the least abundant. Iron-oxide cement is the most common cement type in the sandstones, shales, and siltstones of the Abu Roash “G” Member in the Abu Sennan area. In the Lower Abu Roash “G” Member, the iron-oxide cement is clearly observed in the shale and silty shale of the SWS-21 well (Fig. 4b), in addition to quartz wacke and lithic graywacke of the NWS-1 × well (Fig. 4d). Also, the silty shale and sandy shale present in the GPT-1 well of the Middle Abu Roash “G” Member is marked by this cement type. The same features are present also in the sandy shale of the Upper Abu Roash “G” Member present in the GPT-2 and NWS-1 × wells, in addition to the quartz arenite present in the GPT-1 well (Fig. 4i). Generally, the cementation process starts in the early stages of diagenesis (eodiagenesis, Table 2) and reaches to its maximum role in the later stages (telodiagenesis, Table 2).

Neomorphism

Neomorphism is the process by which the crystal morphology is changed without a major change in the mineral composition (Folk 1965). As the temperature and pressure increase with

burial depth, micro-granular and fine minerals can transform into coarse textures without change in chemical composition. On the other hand, some existing minerals may be completely transformed or changed into a new mineral (eodiagenesis, Table 2). In most of the studied sandy calcareous shale of the Lower Abu Roash “G” Member present in the GPY-1 well, the micritic calcite matrix is partially affected by aggrading neomorphism and replaced by micro- and pseudo-spars. The pack/wackstone of SWS-21 well is marked by allochemical components embedded in partially crystallized micritized calcite (telodiagenesis; Fig. 4a and Table 2).

Depositional setting

The paleogeography of the Upper Cretaceous deposits (Cenomanian to Coniacian) across the present-day Egyptian coastline and just before the Santonian-Maastrichtian transgression is subdivided into inner shelf, outer shelf, slope, and basinal environments (Fig. 5, Tassy et al. 2015). Outer shelf is large in the Nile Delta area and narrower offshore in the Western Desert and the North Sinai areas, limited by normal faults and/or slide scars. It is dominated by mudstone, wackestone, and gypsum. Ali et al. (1989) suggested a shallow marine environment prevailed with paleo-water depth 1–50 m for the Abu Roash “G” Member, in the north Western Desert. In Abu Sennan area, the previously mentioned microfacies association of the Abu Roash “G” Member supports the shallow marine continental–shelf depositional environment.

The deterministic facies model (Fig. 6a–c) depending on the geological geo-bodies was constructed for the sand layer in the three units of Abu Roash “G” to display shallow

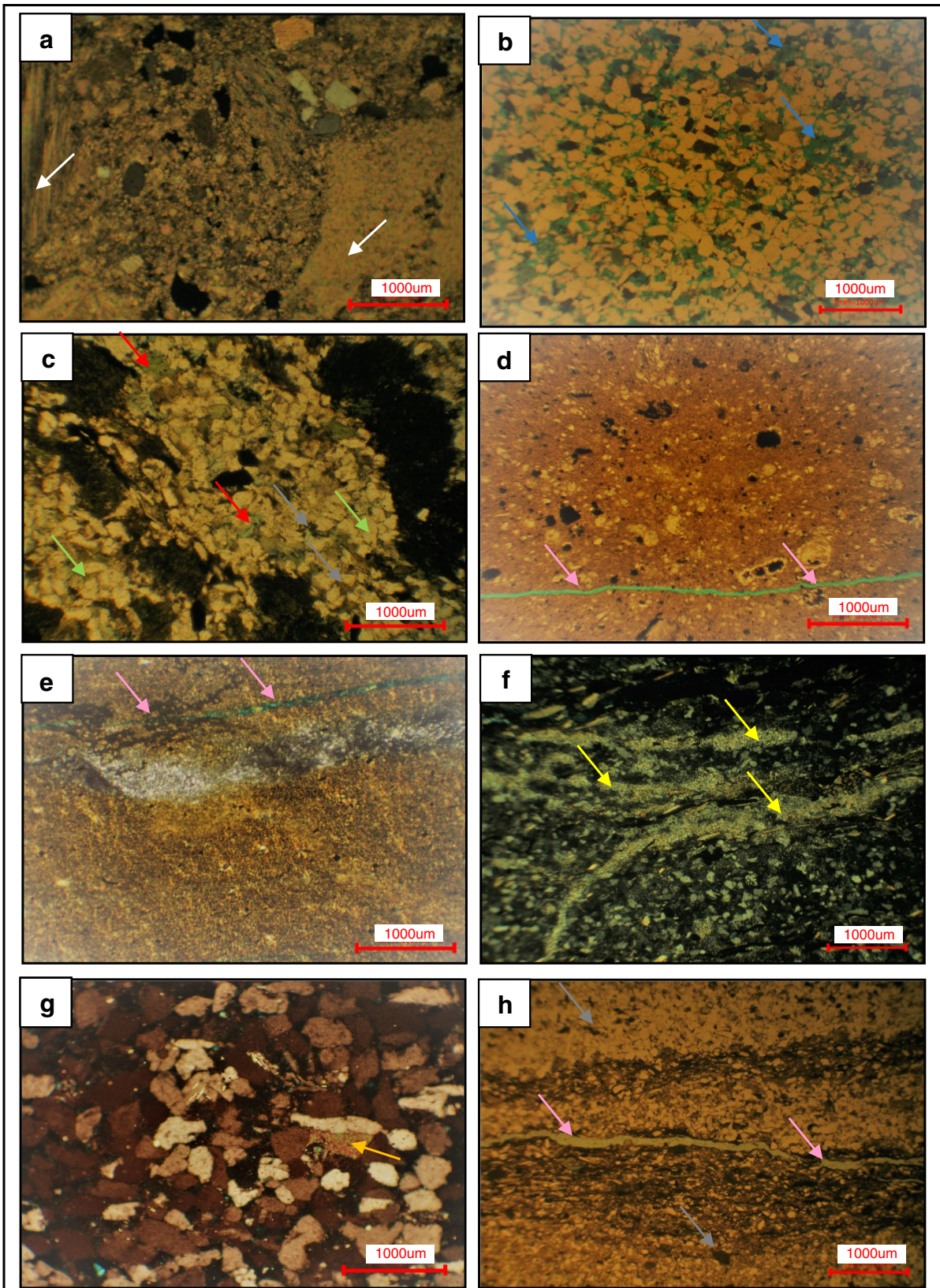


Fig. 4 Microfacies associations of the Abu Roash “G” Member. (a) Pack/wackstone (CN, SWS-21 well), (b) quartz arenite (CN, SWS-21 well), and (c) lithic graywacke (PPL, NWS-1× well) of the Lower Abu Roash “G” Member, (d) calcareous shale (PPL, GPT-1 well) of the Middle Abu Roash “G” Member. (e) Shale, (f) sandy shale, (g) quartz arenite (CN, GPT-2 well), and (h) sandy shale (PPL, NWS-1× well) of the Upper Abu Roash “G” Member

marine continental–shelf depositional environment. This model indicates amalgamated tidal channels for the Lower and Middle Abu Roash “G” sandstone (Fig. 6a) parallel to the NE-SW Jurassic faults (perpendicular to the Cretaceous shoreline, Fig. 5a, b). This model suggests high detrital influx during the upper Abu Roash “G” deposition which may indicate shore face deposition (Fig. 6c) because of the dominance of clastic facies (sandy shale, shale, and quartz arenite).

Cant (1992), on the interpretation of the gamma ray log response (Fig. 7), revealed that the finning upward (bell shape) log behavior (Fig. 8) of the Abu Roash “G” sandstone

Table 2 Diagenetic sequence of the studied microfacies in the Sennan area

Stages of diagenesis			Processes of diagenesis
Telodiagenesis	Mesodiagenesis	Eodiagenesis	
		X	Biogenic alteration
X		X	Cementation
X		X	Neomorphism
X		X	Dissolution
	X		Compaction

The bold letters means the main diagenetic stage

in the studied wells. This supports the presence of the constructed tidal channel in the deterministic facies models (Fig. 6). The histograms of the deterministic facies model show excellent results (Fig. 9) by comparing the well logging, upscaled well logs, and model outputs.

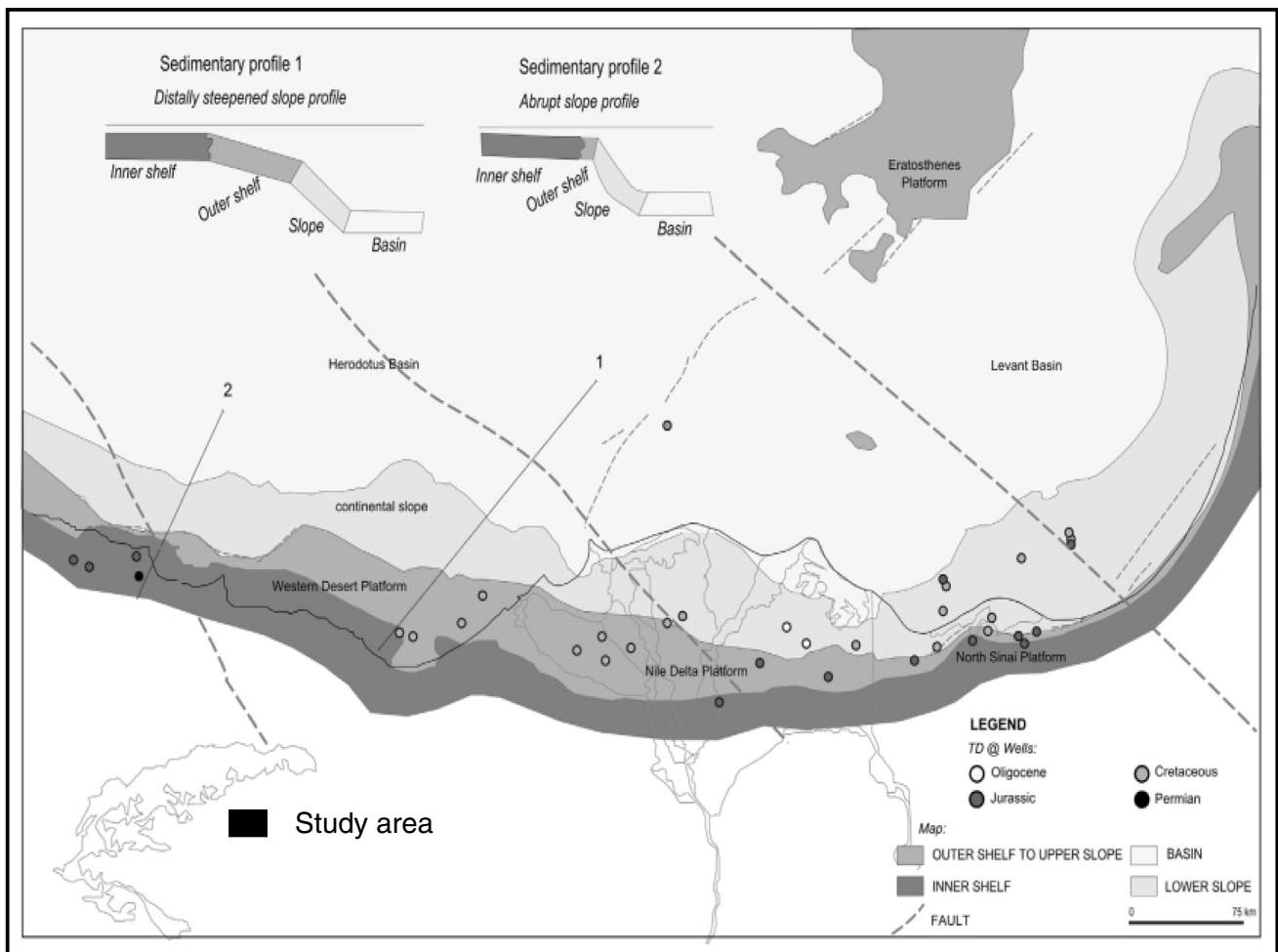
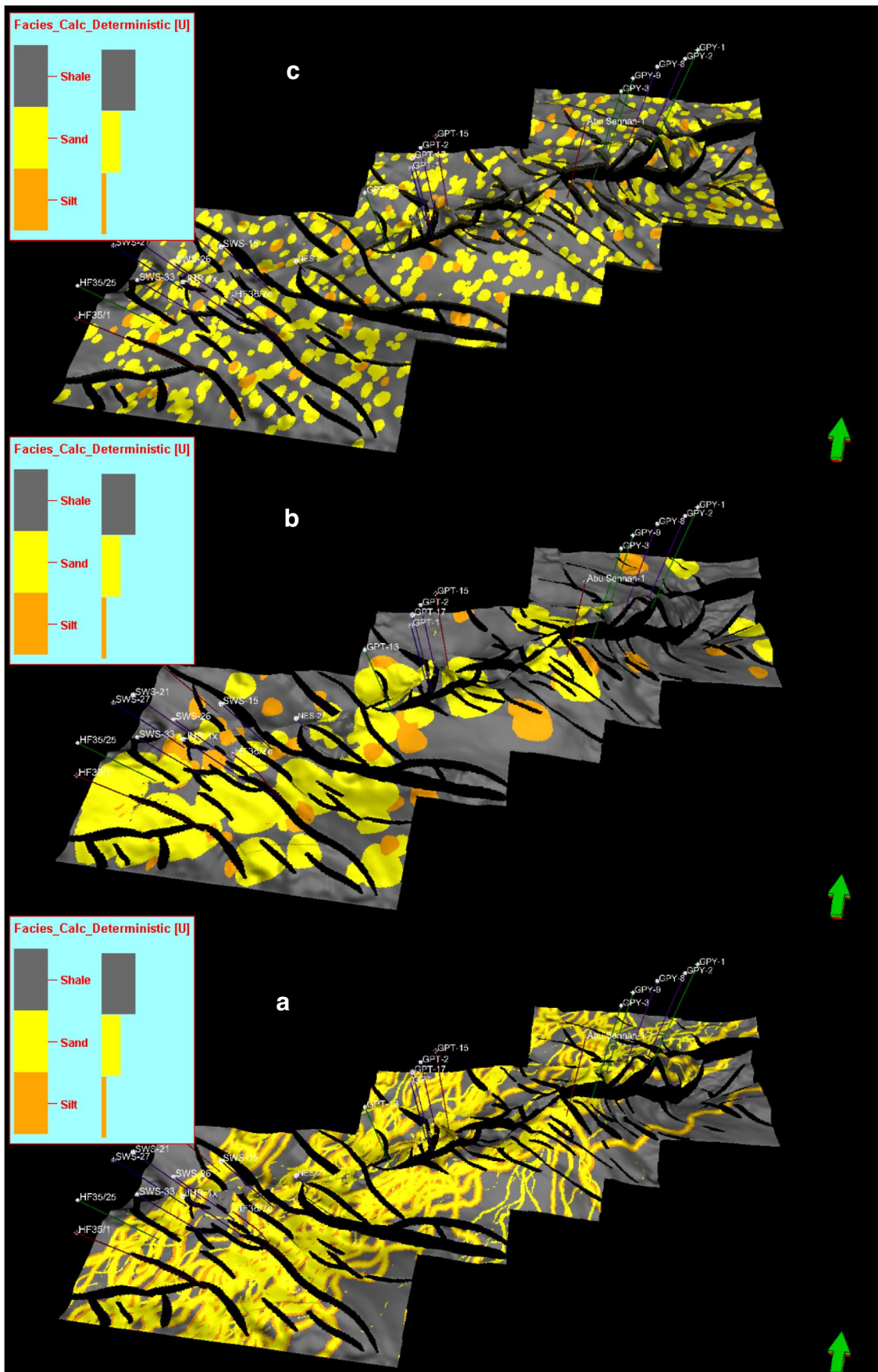


Fig. 5 Paleogeographic map for the Late Cretaceous interval of the Egyptian-Levantine margins (Tassy et al. 2015)



◀**Fig. 6** Deterministic facies modeling of the Abu Roash “G” sand layer in: (a) Lower Abu Roash “G”, (b) Middle Abu Roash “G”, and (c) Upper Abu Roash “G”

Petrophysical evaluation and reservoir assessments

Table 3 shows the porosity and permeability values of the Abu Roash “G” Member in the GPT-1 well. The porosity ranges from 15.9 to 32.9% with an average value of 23.8%, and the horizontal permeability ranges from 0.04 to 254 mD with an average value of 58 mD.

The relation of porosity vs. permeability of the Abu Roash “G” Member (Fig. 10) is expressed by the following equation:

$$K = 1E - 05e^{0.527PHI} \quad r = 0.93, \tag{1}$$

The high values of the correlation coefficients (*r*) revealed that the equations are reliable to a great extent to predict permeability precisely from porosity for layer of the Abu Roash “G” Member in the GPT-1 well.

Some attempts to define the reservoir flow units such as *r*₃₅. It is defined as the pore aperture corresponding to a mercury saturation of 35% pore volume of the mercury injection curve. The term was introduced by Winland who developed an empirical relationship among porosity, air permeability, and pore aperture (*r*₃₅) corresponding to a mercury saturation of 35% for a mixed suit of sandstones and carbonates. The Winland’s equation was used and published by Kolodzie (1980).

$$\log r_{35} = 0.732 + 0.588 \log k_{air} - 0.864 \log \phi \tag{2}$$

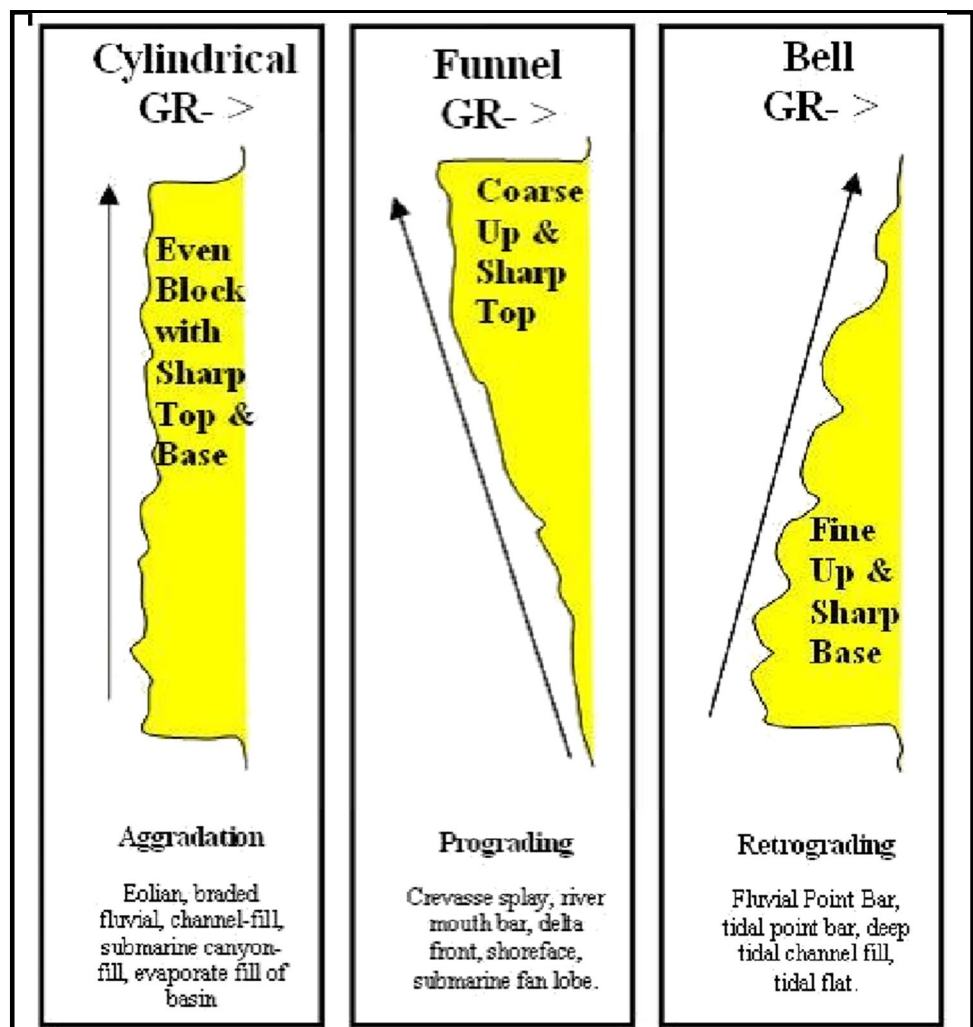
where:

*r*₃₅ pore throat radius equivalent to 35% saturation of mercury, μm.

*k*_{air} sample permeability

mD φ sample porosity, %

Fig. 7 Gamma-ray log behavior showing the depositional environments (Cant 1992)



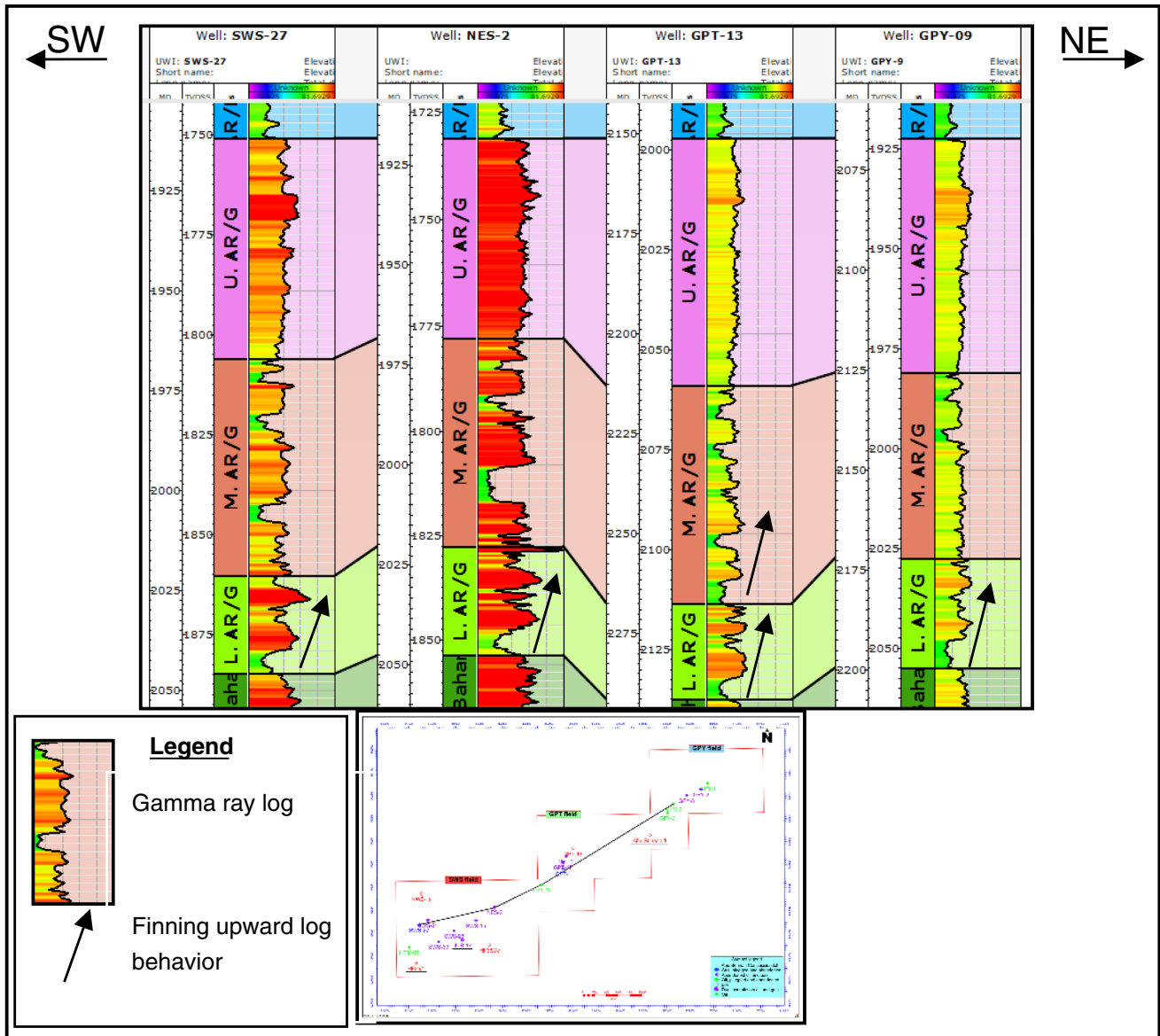


Fig. 8 Gamma-ray log behavior of the Abu Roash “G” Member showing fining upward (bell shape) pattern indicating tidal channel

The Winland’s equation is a strong method to determine the different rock types in a reservoir. Also, the Winland’s plot helps petrophysicists and engineers to understand the properties of the reservoirs rocks (Al-Qenae and Al-Thaqafi 2015).

The flow units can be identified from the calculation of the pore throat radii (r35) using the Winland’s equation, hence four petrophysical flow units with different reservoir performances are distinguished (Martin et al. 1997) as follows:

1. Megaport unit, where r35 value above 10 μm ,
2. Macroport unit, where r35 value ranges between 10 and 2 μm ,
3. Mesoport unit, where r35 value ranges between 2 and 0.5 μm ,

4. Microport unit, where r35 value is less than 0.5 μm .

The plot of the flow units’ identification using Winland flow lines of the Abu Roash “G” Member core samples (Fig. 11) shows that these member samples are marked by three flow units; microport, mesoport, and macroport.

Porosity evaluation versus petrophysical flow units

The Abu Roash “G” Member is marked by two types of porosity, dissolution, and fractures. The dissolution porosity is an important role in quartz arenite of the Lower Abu Roash “G” Member present in the SWS-21 well. The calcareous shale of the Middle Abu Roash “G” Member present in

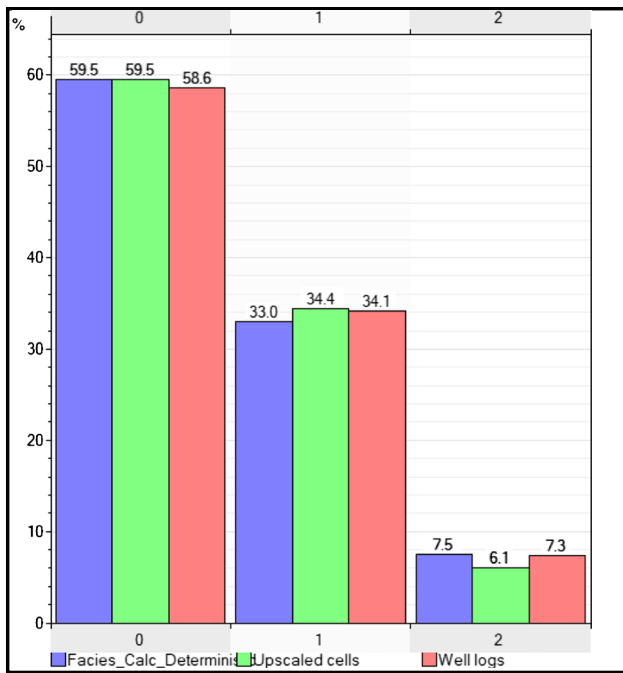


Fig. 9 Histogram of the Abu Roash "G" deterministic facies model

the GPT-1 well, in addition to the sandy shale of the Upper Abu Roash "G" Member present in the NWS-1 x well are marked by fractures which are enhanced by dissolution. This porosity type can be observed in the quartz arenite (GPT-2 well) of the Upper Abu Roash "G" Member.

The petrographical description of the Abu Roash "G" samples confirmed with the petrophysical results in terms of the presence of three flow units within the studied samples

Fig. 10 Porosity vs. permeability of the Abu Roash "G" Member core samples and GPT-1 well of the GPT field

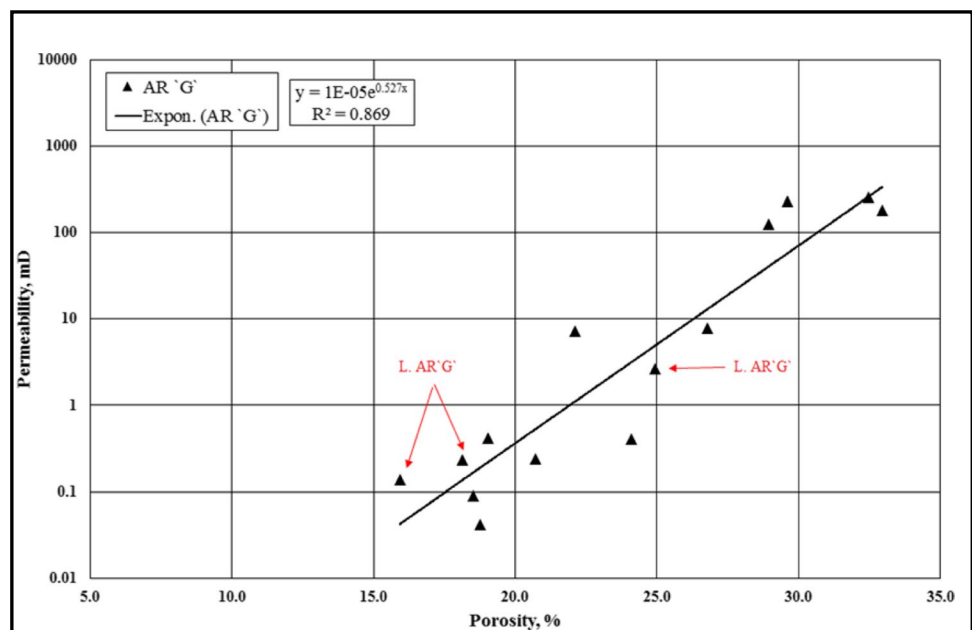


Table 3 The porosity and permeability of the Abu Roash "G" core samples

Formation	Depth m	Sample no	φ%	K mD
Abu Roash "G"	1778.00	1	18.5	0.09
	1778.25	2	29.6	228
	1780.00	3	22.1	7.2
	1780.25	4	20.7	0.24
	1781.00	5	28.9	124
	1781.25	6	19.0	0.41
	1782.25	7	18.8	0.04
	1783.00	8	26.8	7.8
	1783.25	9	24.1	0.41
	1799.00	10	32.5	254
	1799.25	11	32.9	183
	1874.00	12*	24.9	2.6
	1876.00	13*	18.1	0.23
	1876.25	14*	15.9	0.14

*Samples of the Lower Abu Roash "G".

(Fig. 12). The sample that represents the microport flow unit group (Fig. 12a) is characterized by the highest cemented nature accompanied with the confined pore spaces (blue color) between the grains. They connected through narrow throats for flow; consequently, the tight flow regime is expected for this system. The sample that represents the mesoport unit group (Fig. 12b) shows slight improvement in terms of volumes of pore throat and pore body; hence the flow property improvement is expected. Regarding macroport flow unit (Fig. 12c), it displays low cemented nature (connected pore spaces, blue color) between the

Fig. 11 The flow units of the Abu Roash “G” Member core samples using Winland flow lines and GPT-1 well of the GPT field

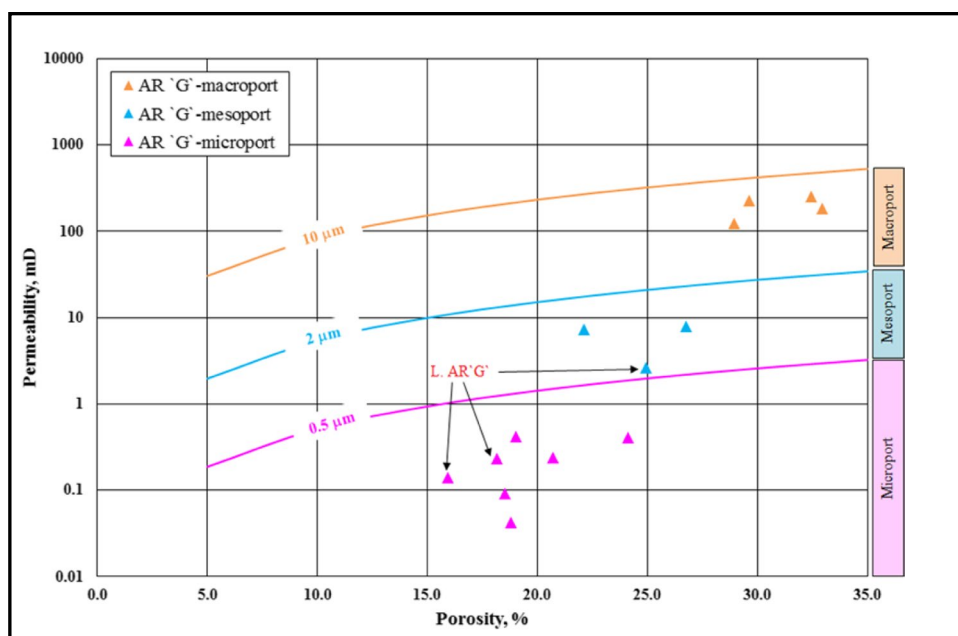
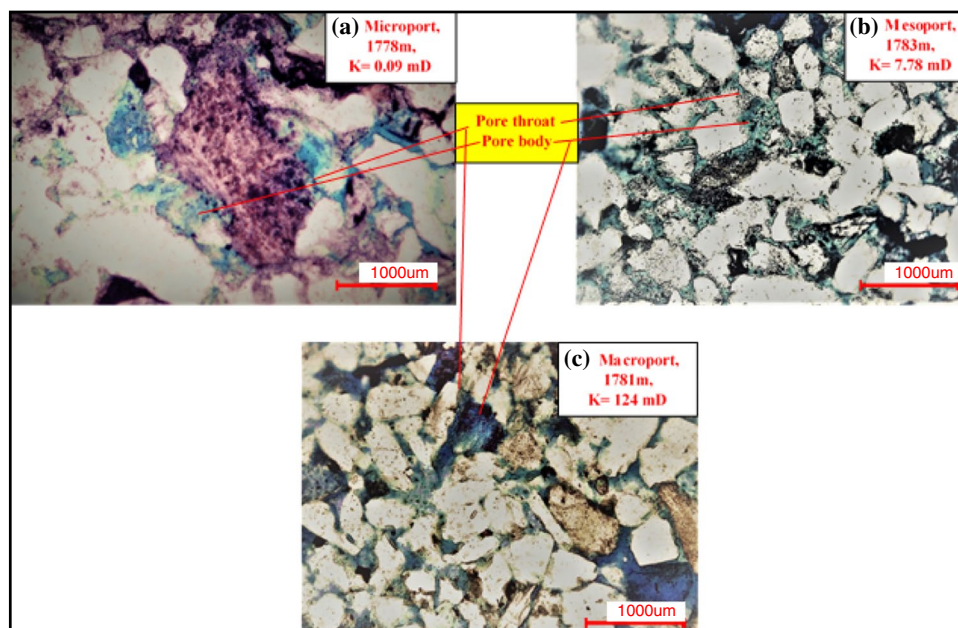


Fig. 12 Composite photomicrograph displaying the petrographic aspects and distinctive pore system for the different flow units within the Abu Roash “G” studied samples, which are characterized by quartz arenite microfacies where, (a): microport pore system represented by blue color, S#1, 1778 m, PPL. (b) Mesoport pore system represented by blue color, S#8, 1783 m, PPL. (c) Macroport pore system represented by blue color, S#5, 1781 m, PPL



grains. Hence, the extensive flow is the distinctive attribute for this system.

Conclusion

The Late Cenomanian Abu Roash “G” Member is an important oil/gas reservoir in Abu Sennan area, north Western Desert, Egypt. It is subdivided into the lower, middle, and

upper units. The lower and middle units are formed of clastic and carbonate facies. The lower and middle unit is formed of clastic and carbonate facies. The lower unit is marked by quartz wacke and lithic grey wacke in the side wall core of the NWS-1x well; pack-wackstone, shale, silty shale and quartz arenite in the SWS-21 well; quartz arenite and sandy calcareous shale in the HF36/7E and GPY-1, respectively, while, the investigated microfacies of the middle unit are calcareous shale, silty shale and sandy shale in the GPT-1 well.

On the other hand, the upper unit is dominated by clastic microfacies (sandy shale in the side wall core of the NWS-1x well; shale, sandy shale, and quartz arenite in the GPT-2 well; quartzarenite in the GPT-1 well).

The dissolution process enhanced the fracture and formed channel porosity which sometimes may be filled by silica during late stages of diagenesis. The Abu Roash “G” in the study area is a typical analogue for this reservoir in the Abu Gharadig basin of the Western desert, as there is no wide lateral facies change.

The microfacies association of the Abu Roash “G” Member supports shallow marine environment. This model indicates amalgamated tidal channels for the Lower and Middle Abu Roash “G” sandstone (perpendicular to the Cretaceous shoreline). Also, this model suggests high detrital influx during the Upper Abu Roash “G” deposition which may indicate shore face deposition. Dissolution and compaction are the most effective diagenetic processes which enhance porosity of the Abu Roash “G” reservoir.

The textural and mineralogical characteristics of Abu Roash “G” Member revealed the heterogeneities of this member as a result of its depositional setting and diagenesis. Petrophysically, the Abu Roash “G” Member is a heterogeneous reservoir in the GPT-1 well in terms of flow properties, where three flow units with different capabilities are involved. Reservoir performance would be different among the contained microport, mesoport, and macroport flow units. The petrographical description of the Abu Roash “G” samples is confirmed with the petrophysical results in terms of the presence of these flow units within the studied samples. The microport flow unit group is characterized by a tight flow regime as a result of high cementation, confined pore spaces, and narrow pore throats. The mesoport unit group shows slight improvement in the volume of pore throats and pore bodies; hence, the flow property improvement is expected. The macroport flow unit displays low cemented nature and spacious pore spaces with wide pore throats; hence, the extensive flow is the distinctive attribute for this system. The porosity and permeability results of the Abu Roash “G” reservoir need to be improved by more investigated core samples which could be taken from the future drilled wells.

Declarations

Conflict of interests The authors declare no competing interests.

References

- Abdel Gawad E, Fathy M, Ali MM (2016) Characterizations of the Late Cenomanian reservoirs, El Diyur field, north Western Desert. *Egypt J Appl Geol Geophys* 4:47–59
- Abdel Wahab AA, Turner I (1991) Diagenesis of the Nubia Formation, Central Eastern Desert. *Egypt J Afr Earth Sci Middle East* 13:343–358
- Ali SM, Basher G, Ammar G (1989) Razzak oil field stratigraphic study: GUPCO’s unpublished internal report, p. 1–16
- Al-Qenae KJ, Al-Thaqafi SH (2015) New approach for the classification of rock typing using a new technique for iso-pore throat lines in Winland’s Plot. *Soc Pet Eng*
- Baiyegunhi C, Liu K, Gwavava O (2017) Geochemistry of sandstones and shales from the Ecca Group, Karoo Supergroup, in the Eastern Cape Province of South Africa, implications for provenance, weathering and tectonic setting. *Open Geosci J* 9:340–360
- Bekhit M, Mohamed M, Fathy M (2017) Facies analysis of Abu Roash (G) Member and Upper Bahariya Formation of Asala-Samra Oil Fields. North Western Desert, Egypt. <https://doi.org/10.7537/marsnsj151117.18>
- Bjørlykke K, Jahren J, Mondol NH, Marcussen O, Croize D, Christer P, Thyberg B (2009) Sediment compaction and rock properties. AAPG International Conference and Exhibition
- Burley SD, Kantorowicz JD (1986) Thin section and S.E.M. textural criteria for the recognition of cement-dissolution porosity in sandstones. *Sedimentology* 33:587–604
- Cant DJ (1992) Subsurface facies analysis in facies models-response to sea level change. Walker, R. G. and James, N. P., eds.: *Geological Association of Canada*, p. 27–45
- Choquette PW, Pray LC (1970) Geologic nomenclature and classification of porosity in sedimentary carbonates. *Am Assoc Pet Geologists Bull* 54:207–250
- Dunham RJ (1962) Classification of carbonate rocks according to depositional texture, in *Classification of carbonate rocks*, W.E. Ham (Ed.). American Association of Petroleum Geologists Memoir No. 1, Tulsa, OK, p. 108–121
- Farrag GH (2021) Hydrocarbon potentiality of Abu Sennan blocks, Western Desert, Egypt. Ph.D Thesis (2021), Geology Department, Ain Shams University
- Farrag GH, Bakr A, Abdallah A, El-Shahawy S (2021) Seismic criteria and structural styles for half graben differential inversion, implication for hydrocarbon accumulations, Abu Sannan blocks, Western Desert Egypt. *Environm Geo Sci* 28(1):33–42
- Farrag GH, Baghdady A, ElNaggar OM (2021) Petrophysical attributes of the middle zone of the Bahariya as a producing reservoir using core analysis correlations and log evaluation, Abu Sennan area Egypt. *Afr Earth Sci* 180(2021):104225
- Farrow GE, Fafe JA (1988) Bio-Erosion and Carbonate Mud Production on High Latitude Shelves. *Sediment Geol* 60:281–297
- Folk RL (1965) Some aspects of recrystallization in ancient limestones, in *dolomitization and limestone diagenesis*, L. C. Pray and R. C. Murray (Eds.): SEPM special publication No. 13, p. 14–48
- GPC Internal Report (1980) Geological study of Abu Sennan area, Western Desert, Egypt, unpublished
- Kolodzie SJR (1980) Analysis of pore throat size and use of the Waxman-Smits equation to determine OOIP in Spindle field, Colorado: Society of Petroleum Engineers, 55th Annual Fall Technical Conference, Paper SPE-9382, 10 p
- Martin AJ, Solomon ST, Hartmann DJ (1997) (1997) Characterization of petrophysical flow units in carbonate reservoirs. *Am Assoc Pet Geologists* 81(5):734–759
- Morad S, Ketzer JM, De Ros LF (2000) Spatial and temporal distribution of diagenetic alterations in silici-clastic rocks: implications for mass transfer in sedimentary basins. *Sedimentology* 47:95–120
- Pasley MA, Artigas G, Nassef O, Comisky J (2009) Depositional facies control on reservoir characteristics in the Middle and Lower Abu Roash “G” Sandstones, Western Desert, Egypt: American Association of Petroleum Geologists Conference and Exhibition South Africa, Article #5018
- Pettijohn FJ, Potter PE, Siever R (1987) *Sand and sandstones*, 2nd edn. Springer-Verlag, New York, p 559

- Pittman ED (1979) Porosity, diagenesis and productive capability of sandstone reservoirs. *SEPM, Special Publication 26*:159–173
- Sultan A, Hanafy S, Saleh A, Eid E, El-Srougy S (2019) The impact of depositional facies control and reservoir characteristics in the middle Abu Roash “G” sandstones on Reserve Estimation, East Abu Sennan Concession, Western Desert, Egypt. (East Abu Sennan Discovery and Challenges): Paper presented at the Offshore Mediterranean Conference and Exhibition, Ravenna, Italy, March 2019. Paper Number: OMC-2019–0881 Published: March 27 2019
- Tassy A, Crouzy A, Gorini C, Rubino JL, Bouroullec J, Sapin F (2015) Egyptian Tethyan margin in the Mesozoic, evolution of a mixed carbonate-siliciclastic shelf edge (from Western Desert to Sinai). *Mar Pet Geol* 3:1–157
- Osman WM, Abdel Gawad A, Mesbah MA, Abdel Fattah ThA (2017) Application of well logging and seismic techniques for evaluation of hydrocarbon potentialities, East Abu Sennan area, Western Desert Egypt. *Int J Sci Eng Appl Sci* 3:42–86
- Worden RH, Burley SD (2003) Sandstone diagenesis. Recent and ancient. <https://doi.org/10.1002/9781444304459>